Available online at www.sciencedirect.com
SCIENCE DIRECT®
Journal of Solid State Chemistry 179 (2006) 169–174
JOURNAL OF SOLID STATE CHEMISTRY
www.elsevier.com/locate/jssc

High-pressure synthesis and crystal structure analysis of $NaMn_2O_4$ with the calcium ferrite-type structure

Junji Akimoto[a,*], Junji Awaka[a], Norihito Kijima[a], Yasuhiko Takahashi[a], Yuichi Maruta[b], Kazuyasu Tokiwa[b], Tsuneo Watanabe[b]

[a]*National Institute of Advanced Industrial Science and Technology (AIST), 1-1-1 Higashi, Tsukuba, Ibaraki 305-8565, Japan*
[b]*Department of Applied Electronics, Tokyo University of Science, 2641 Yamazaki, Noda, Chiba 278-8510, Japan*

Received 31 August 2005; received in revised form 12 October 2005; accepted 17 October 2005
Available online 15 November 2005

Abstract

Single crystals of a new sodium manganese oxide, $NaMn_2O_4$, were synthesized for the first time using a high-temperature and high-pressure technique. The $NaMn_2O_4$ single crystal is black, has a needle shape, and crystallizes in the orthorhombic calcium ferrite-type structure, space group *Pnam* with $a = 8.9055(18)$ Å, $b = 11.0825(22)$ Å, $c = 2.8524(5)$ Å, $V = 281.52(9)$ Å^3, and $Z = 4$. The structure was determined from a single-crystal X-ray study and refined to the conventional values $R = 0.041$ and $wR = 0.034$ for 1190 observed reflections. The framework structure is built up from edge-sharing chains of MnO_6 octahedra that condense to form one-dimensional tunnels in which the sodium atoms are located. The Mn–O bond distance and bond valence analyses revealed the manganese valence Mn^{3+}/Mn^{4+} ordering in the two "double rutile" chains of $NaMn_2O_4$.

Keywords: $NaMn_2O_4$; Sodium manganese oxide; Calcium ferrite; High-pressure synthesis; Single-crystal X-ray diffraction; Structure analysis; Charge ordering

1. Introduction

The Mn^{3+}/Mn^{4+} mixed valence ternary oxides display a wide range of interesting properties from lithium insertion/extraction reactions in the spinel-type $LiMn_2O_4$ and the layered rocksalt related-type $LiMnO_2$, to magnetoresistance in doped $AMnO_3$ with the perovskite structure. In $LiMn_2O_4$, the average manganese oxidation state is $+3.5$, that is, there are equal numbers of Mn^{3+} (electronic configuration: $3d^4$; $t_{2g}^3e_g^1$) and Mn^{4+} ($3d^3$; $t_{2g}^3e_g^0$) cations in the structure. The Jahn-Teller distortion of Mn^{3+} plays a crucial role in structural modification. Mn^{3+} and Mn^{4+} cations are randomly distributed at the octahedral site of the spinel structure above room temperature, while they are localized on five independent sites at low temperature [1,2]. On the other hand, the perovskite-type $Pr_{0.5}Sr_{0.5}MnO_3$ with $Mn^{3+}/Mn^{4+} = 1{:}1$ shows a first-order phase transition from a ferromagnetic metal to an antiferromagnetic nonmetal at 140 K, which accompanies the transition to the Mn^{3+}/Mn^{4+} charge-ordered state [3].

Similar M^{3+}/M^{4+} (1:1) mixed-valence compounds, such as the spinel-type $LiTi_2O_4$ [4] and the calcium ferrite-type $NaTi_2O_4$ [5,6] and $NaRu_2O_4$ [7], show interesting physical and structural properties. These compounds have the simple AB_2O_4-type chemical formula, which is one of the major series of complex oxides in solid-state chemistry [8]. Structure analysis reveals that the M^{3+} and M^{4+} cations are randomly distributed amongst the octahedral sites in these compounds.

In the Na–Mn^{3+}–Mn^{4+}–O system, Parant et al. [9] reported six compounds; $Na_{0.20}MnO_2$, $Na_{0.40}MnO_2$, $Na_{0.44}MnO_2$, $Na_{0.70}MnO_2$, and two polymorphs of $NaMnO_2$. Attempts to synthesize the calcium ferrite-type $NaMn_2O_4$ and $NaMnTiO_4$ at ambient pressure failed in earlier studies [8,10]. In fact, heating a mixture of Na_2CO_3 and Mn_2O_3 (1:2) at high temperatures resulted in the production of the $Na_{0.44}MnO_2$ phase [11,12].

Because the calcium ferrite-type structure is the most dense structure for known crystalline materials with AB_2O_4

*Corresponding author. Fax: +81 29 861 9214.
E-mail address: j.akimoto@aist.go.jp (J. Akimoto).

0022-4596/$ - see front matter © 2005 Elsevier Inc. All rights reserved.
doi:10.1016/j.jssc.2005.10.020

stoichiometry, the high-pressure technique appears to be useful for realizing $NaMn_2O_4$. For example, the spinel ($MgAl_2O_4$) transforms to the calcium ferrite-type structure at pressures above 25 GPa [13,14].

In the present study, we report the high-pressure synthesis and crystal structure of a new sodium manganese oxide compound, $NaMn_2O_4$, with the calcium ferrite-type structure.

2. Experimental procedures

Single crystals of sodium manganese oxides were synthesized using a high-pressure technique. The starting materials were Na_2O_2 powder and Mn_2O_3 powder weighted in an atomic ratio of Na/Mn = 1 and mixed in a dry box to avoid absorption of moisture. The mixture was pressed into a pellet and put into a gold capsule, and heated at 1373 K for 5 h under a pressure of 4.5 GPa using a cubic-anvil-type high-pressure apparatus. Details of the experimental conditions were reported in another paper [15]. Chemical compositions of the products were analyzed by SEM-EDX (JEOL JSM-5400) at an acceleration voltage of 20 kV using selected single-crystal specimens. The crystal structure was examined with an X-ray precession camera (Mo $K\alpha$ radiation by a Zr foil) to check on the crystal quality and to determine the lattice parameters, systematic extinctions, and possible superstructures. Integrated intensity data were collected on a Rigaku AFC-7S four-circle diffractometer at 298 K.

3. Results and discussion

3.1. Single-crystal synthesis

The main product of the present high-pressure synthesis was platelet-like $NaMnO_2$ crystals [16] of about $0.5 \times 0.5 \times 0.2\,mm^3$ (maximum), which were grown from the melt in the gold capsule. In addition, small, black needle-shaped crystals of about $0.2 \times 0.03 \times 0.03\,mm^3$ (maximum), as shown in Fig. 1, were also crystallized from the high-temperature solution of $NaMnO_2$. The needle crystals thus obtained were investigated by SEM-EDX (JEOL JSM-5400). The chemical composition was determined to be Na:Mn = 1.0:2.0, which agrees well with the structural formula obtained in the present single-crystal study.

Precession photographs indicate that $NaMn_2O_4$ belongs to the orthorhombic system with the possible space group of *Pnam* or $Pna2_1$. The lattice parameters are very similar to those of $NaTi_2O_4$ [5]. These data lead us to the calcium ferrite $CaFe_2O_4$-type structure. The lattice parameters, determined by a least-squares refinement using the 2θ values of 25 strong reflections in the range 20–30° on the four-circle diffractometer, are $a = 8.9055(18)$ Å, $b = 11.0825(22)$ Å, $c = 2.8524(5)$ Å, $V = 281.52(9)$ Å^3.

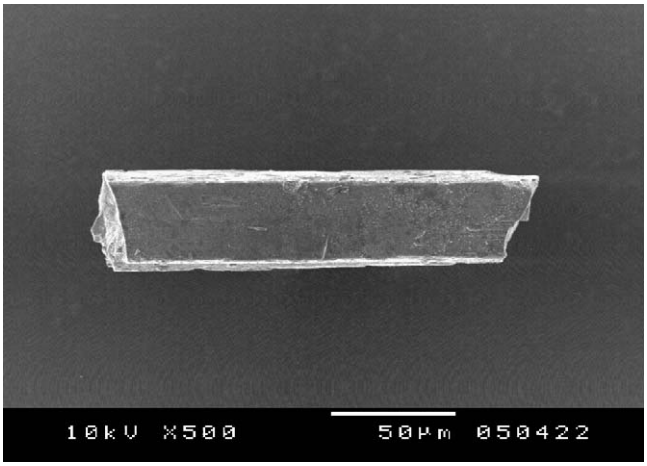

Fig. 1. SEM photograph of $NaMn_2O_4$ single crystal.

3.2. Structure analysis

A small needle crystal, $0.150 \times 0.025 \times 0.025$ mm in size, was used for the structure analysis. The intensity data were collected by the $2\theta - \omega$ scan method with a scan rate of 2°/min at 298 K on the four-circle diffractometer (operating conditions: 50 kV, 30 mA) using graphite-monochromatized Mo $K\alpha$ radiation ($\lambda = 0.71069$ Å). The fluctuations of the intensities, monitored by examining a set of three standard reflections ((320), (040), (002)) taken after every 150 measurements, was within 1.3%. A total of 2111 reflections were obtained within the limit of $2\theta < 110°$. All calculations were carried out using the Xtal3.4 program [17]. Structure factors were obtained after averaging the equivalent Bragg intensities, which were corrected for Lorentz and polarization factors, scale factors, and absorption and extinction effects. Neutral atomic scattering factors for all atoms were applied in the refinement. A summary of the crystallographic and experimental data is given in Table 1.

In the structure analysis that followed, the space group of highest symmetry, *Pnam*, confirmed by successful refinement, was adopted. The refinement was initiated with the reported atomic coordinates for the isostructural compound, $NaTi_2O_4$ [5]. The sodium site deficient model was examined for possible nonstoichiometric character of Na. However, such a model did not improve in both the structural parameters and the R value. Therefore, we proceeded in the structural refinement using the fixed occupancy (100%) for a sodium site. Finally, the crystal structure was refined to $R = 4.1\%$ and $wR = 3.4\%$ for 1190 observed reflections, with a shift/error for all 44 parameters of less than 0.001. The final atomic coordinates and displacement parameters are given in Tables 2 and 3, respectively.

3.3. Structural discussions

The crystal structure of $NaMn_2O_4$ projected down the c-axis direction is shown in Fig. 2. The structure is nearly

Table 1
Crystallographic and experimental summary for $NaMn_2O_4$

Structural formula	$NaMn_2O_4$
Crystal system	Orthorhombic
Space group	*Pnam*
Lattice parameters	
a (Å)	8.9055(18)
b (Å)	11.0825(22)
c (Å)	2.8524(5)
V (Å^3)	281.52(9)
Z	4
D_x (g/cm^3)	4.645
Crystal size (mm)	$0.150 \times 0.025 \times 0.025$
Temperature (K)	298
Maximum 2θ (deg)	110
Absorption correction method	Gaussian integration
Transmission factors	
Min.	0.715
Max.	0.816
Measured reflections	2111
R_{int}	0.021
Independent reflections	1734
Observed reflections ($>4\sigma$)	1190
Number of variables	44
R	0.041
wR[w $= 1/\sigma^2 F$]	0.034
Extinction parameter g	125(9)

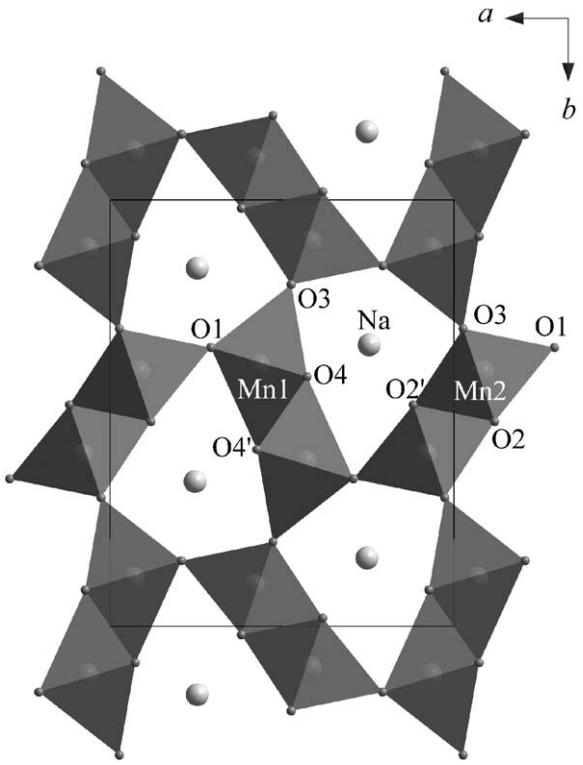

Fig. 2. Crystal structure of $NaMn_2O_4$ viewed along [001]. MnO_6 are illustrated as octahedra, and Na atoms as large balls.

Table 2
Atomic positional and equivalent isotropic displacement parameters for $NaMn_2O_4$

Atom	Site	x	y	z	U_{eq} (Å^2)
Na	4*c*	0.24670(13)	0.33975(10)	1/4	0.0109(5)
Mn1	4*c*	0.06764(6)	0.11327(4)	1/4	0.00691(17)
Mn2	4*c*	0.08285(5)	0.59752(4)	1/4	0.00612(16)
O1	4*c*	0.2925(3)	0.6541(2)	1/4	0.0113(10)
O2	4*c*	0.3817(3)	0.9803(2)	1/4	0.0121(10)
O3	4*c*	0.4735(3)	0.1982(2)	1/4	0.0110(10)
O4	4*c*	0.0729(3)	0.9146(2)	1/4	0.0104(9)

Table 3
Anisotropic displacement parameters[a] for $NaMn_2O_4$

Atom	U_{11}	U_{22}	U_{33}	U_{12}	U_{13}	U_{23}
Na	0.0091(5)	0.0116(5)	0.0121(5)	−0.0020(4)	0	0
Mn1	0.00792(16)	0.00877(17)	0.00405(18)	−0.00212(14)	0	0
Mn2	0.00697(16)	0.00735(15)	0.00404(18)	−0.00062(13)	0	0
O1	0.0090(9)	0.0155(11)	0.0093(10)	0.0017(8)	0	0
O2	0.0151(11)	0.0123(10)	0.0089(10)	−0.0025(8)	0	0
O3	0.0165(11)	0.0077(8)	0.0089(10)	−0.0016(8)	0	0
O4	0.0104(9)	0.0124(9)	0.0084(10)	−0.0020(8)	0	0

[a]Defined as $\exp\{-2\pi^2 \Sigma_{ij} h_i h_j a_i^* a_j^* U_{ij}\}$.

identical to those of the calcium ferrite-type compounds, e.g., $CaFe_2O_4$ [18–20], $NaFeTiO_4$ [21,22], and $NaTi_2O_4$ [5,6]; they have the same space group and similar coordination environments. The basic unit of the $NaMn_2O_4$ structure is the "double rutile" chain [23], in which a pair of edge-shared MnO_6 octahedra piles up along the *c*-axis with sharing edges. Four chains are linked by sharing vertices to form a three-dimensional framework structure (Fig. 3) and produce a single tunnel elongated to the *c*-axis, in which the sodium atoms are located. The selected bond distances are listed in Table 4.

In most of the calcium ferrite-type $NaM^{3+}M^{4+}O_4$ (M = Fe, Sc, Ti, Sn, Ru, Rh, etc.) compounds [5,7,21,22,24], two octahedral sites are randomly occupied by M^{3+} and M^{4+} cations. Therefore, octahedral coordination environments of two double rutile chains are very similar to each other in these compounds. In contrast, the most characteristic feature in the present $NaMn_2O_4$ structure is the manganese valence ordering in the two Mn sites. As listed in Table 4, both Mn1 and Mn2 atoms are octahedrally coordinated by six oxygen atoms. However, the coordination environments of oxygen atoms around the Mn1 and Mn2 atoms are apparently different from one another. In the $Mn1O_6$ octahedron, there are two long axial Mn1–O bonds of 2.252(2) Å and 2.202(2) Å, and two equatorial pairs at 1.947(2) Å and 1.922(2) Å, and the average Mn1–O distance is 2.032 Å. Therefore, the local environment of the Mn1–O octahedron is distorted significantly, such as in the Mn^{3+}–O compounds, e.g., $LiMnO_2$ [16,25,26] and $NaMnO_2$ [16]. This fact can be explained by the preferential occupation of the Jahn-Teller Mn^{3+} ion at the Mn1 site. On the other hand, the Mn2–O distance varies in the short range of 1.879(2)–1.988(3) Å

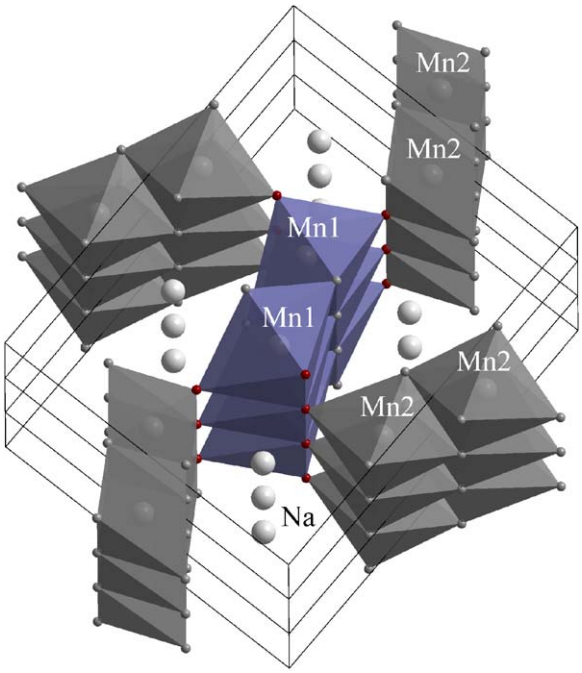

Fig. 3. Four corner-sharing linkages of double chains in $NaMn_2O_4$. Oxygen atoms at the corners of the central Mn1 double chain are emphasized.

Table 4
Selected bond distances (Å) for $NaMn_2O_4$

Na–O1	2.527(2) × 2	Mn1–O1	1.947(2) × 2
Na–O2	2.402(2) × 2	Mn1–O3	2.252(2)
Na–O3	2.558(3)	Mn1–O4	1.922(2) × 2
Na–O3′	2.469(3)	Mn1–O4′	2.202(2)
Na–O4	2.303(2) × 2	Mean	2.032
Mean	2.436		
		Mn2–O1	1.969(3)
Mn1–Mn1	2.8524(5)	Mn2–O2	1.955(2) × 2
Mn1–Mn1′	3.1288(7)	Mn2–O2′	1.988(3)
Mn2–Mn2	2.8524(5)	Mn2–O3	1.879(2) × 2
Mn2–Mn2′	2.9806(7)	Mean	1.938

(Table 4). The average Mn2–O distance is 1.938 Å, which is much shorter than the Mn1–O distance. These facts suggest the manganese valence Mn^{3+}/Mn^{4+} ordering in the two "double rutile" chains of $NaMn_2O_4$ (Fig. 3). In fact, the calculated valence state of Mn1 (+3.1) is smaller than that of Mn2 (+3.7) using a valence bond analysis [27]. It should be noted that the average Mn–O distance (1.985 Å) in $NaMn_2O_4$ is well consistent with that in the spinel-type $LiMn_2O_4$, the value of which is 1.959 Å [28].

The sodium atom is surrounded by eight oxygen atoms in a bicapped trigonal prism at an average of 2.436 Å, as shown in Fig. 4, which is very consistent with the reported values of 2.481 Å in $NaTi_2O_4$ [5] and 2.431 Å in $NaRh_2O_4$ [24]. This coordination type is normal for sodium atoms in the calcium ferrite-type structure. However, the Na–O4 distance (Table 4 and Fig. 4) is much shorter than the other Na–O distances, the value of which is 2.303(2) Å. As a result, the tunnel shape in the present $NaMn_2O_4$ is slightly distorted, in comparison with those in the "normal" calcium ferrite-type compounds. This fact can be explained by the difference in the distortion between the Mn1 and Mn2 double chains (Fig. 2).

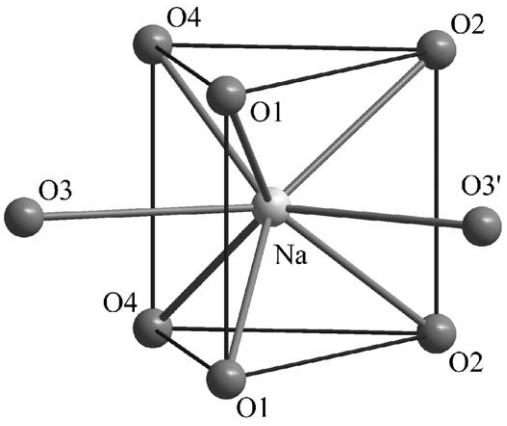

Fig. 4. Na–O coordination in $NaMn_2O_4$.

Table 5
Crystal data for the calcium ferrite related-type compounds

Compounds	Crystal system	Space group	Lattice parameters		
			a (Å)	*b* (Å)	*c* (Å)
$CaFe_2O_4$	Orthorhombic	*Pnam*	9.230	10.705	3.024
$CaMn_2O_4$	Orthorhombic	*Pmab*	9.677	9.988	3.155
$CaTi_2O_4$	Orthorhombic	*Bbmm*	9.718	9.960	3.140

3.4. Structural features in the related compounds

$NaTi_2O_4$ [5] and the present $NaMn_2O_4$ are isostructural to the calcium ferrite $CaFe_2O_4$, which crystallizes in the same space group, *Pnam*, and has similar lattice parameters $a = 9.230$ Å, $b = 10.705$ Å, $c = 3.024$ Å [19,20] (Table 5). On the other hand, mineral marokite, $CaMn_2O_4$, having the similar lattice parameters $a = 9.677$ Å, $b = 9.988$ Å, $c = 3.155$ Å with the space group *Pmab*, was reported in the literature [29–32]. The structure of $CaMn_2O_4$ (Fig. 5) was originally determined in 1964 [29,30] and was recently refined using synthetic single crystal samples [31,32]. Both $CaFe_2O_4$ and $CaMn_2O_4$ structures are made up of "double chains," but the connectivity of these chains differs. Namely, two edge-sharing and two vertex-sharing linkages of double chains are constructed in $CaMn_2O_4$ (Fig. 6), while four vertices of the double chains are shared in the $CaFe_2O_4$ structure (Fig. 3). Accordingly, in $CaMn_2O_4$, there is one unique Mn site, which is on a general position. The average equatorial Mn–O distance is 1.922 Å, and the elongated axial bonds are 2.366 and 2.464 Å, respectively [31]. The elongated Mn–O bonds are due to the Jahn-Teller distortions expected for high-spin d^4 systems, and the

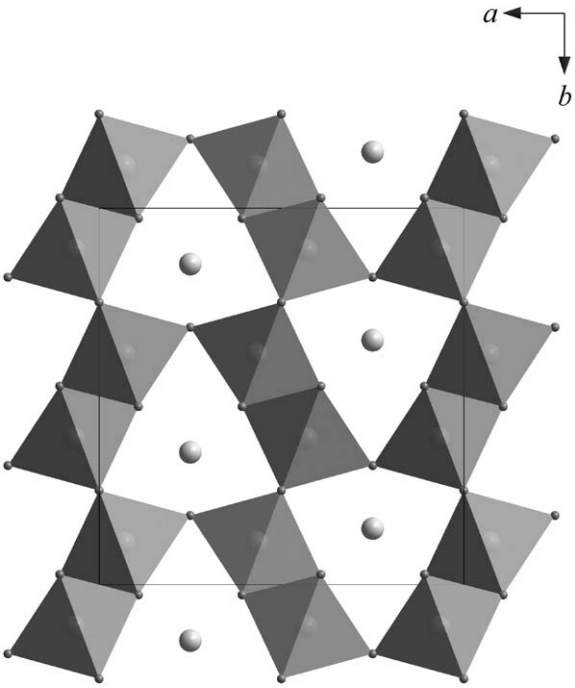

Fig. 5. Crystal structure of $CaMn_2O_4$ viewed along [001]. MnO_6 are illustrated as octahedra, and Ca atoms as large balls.

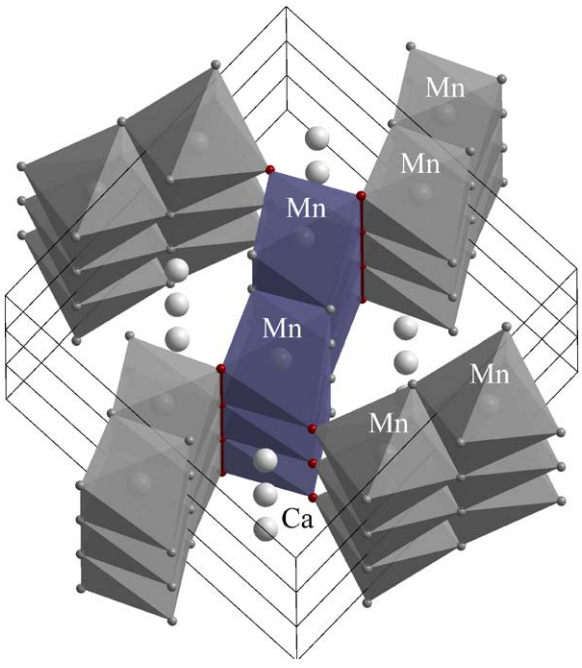

Fig. 6. Two corner- and two edge-sharing linkages of double chains in $CaMn_2O_4$. Oxygen atoms at the corners and O–O edges of the central Mn double chain are emphasized.

situation is consistent with that for Mn1–O bonds in the present $NaMn_2O_4$. It should be noted, however, that there is a difference in the elongation directions. The $Mn1O_6$ octahedron elongates to the *b*-axis direction in the present $NaMn_2O_4$ (Fig. 7a), while the MnO_6 octahedron elongates

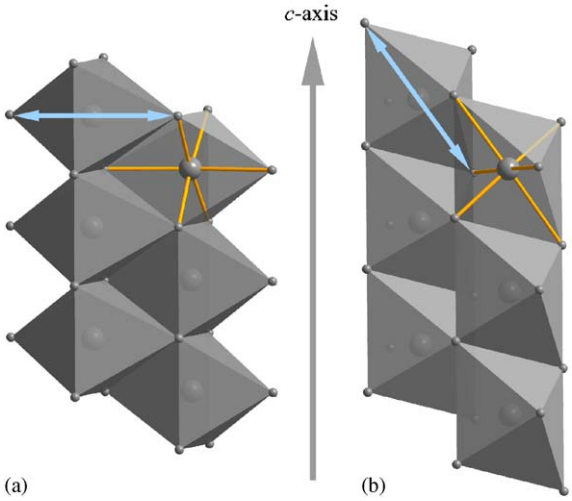

Fig. 7. Two Mn^{3+}–O double chains along the *c*-axis direction: (a) the Mn1 chain in $NaMn_2O_4$ and (b) the Mn chain in $CaMn_2O_4$. The elongation directions of the $Mn^{3+}O_6$ octahedra are indicated by arrows.

to the approximately *c*-axis direction in $CaMn_2O_4$. (Fig. 7b)

Another related compound, $CaTi_2O_4$, also has the similar orthorhombic lattice parameters $a = 9.718$ Å, $b = 9.960$ Å, $c = 3.140$ Å [33,34] (Table 5), and the linkages of double chains are quite similar to those in $CaMn_2O_4$ (Fig. 5). However, $CaTi_2O_4$ crystallizes in another space group, *Bbmm* [33,34]. This may be related to degrees of the $M^{3+}O_6$ octahedral distortion in these compounds. In fact, the Ti–O distance varies in the short range of 1.961–2.135 Å in $CaTi_2O_4$ [34], which gives an average Ti–O distance of 2.067 Å. This value is consistent with the reported Ti^{3+}–O distance, e.g., 2.079 Å in $NaTiO_2$ [35] and 2.048 Å in Ti_2O_3 [36]. Accordingly, the shape of the "double rutile" chain in $CaTi_2O_4$ is scarcely distorted and is quite similar to that in the Mn2–O chain in the present $NaMn_2O_4$.

4. Conclusion

A new member of the calcium ferrite-type structure, $NaMn_2O_4$, was synthesized under high pressure of 4.5 GPa. Small, black needle-shaped $NaMn_2O_4$ crystals were grown from the high-temperature solution of $NaMnO_2$. The crystal structure was determined by the single-crystal X-ray diffraction method. The Mn–O bond distance and bond valence analyses revealed the manganese valence Mn^{3+}/Mn^{4+} ordering in the two "double rutile" chains of $NaMn_2O_4$. This is the first example of the valence ordering in the calcium ferrite-type $NaM^{3+}M^{4+}O_4$ compounds. We are now trying to synthesize the $NaMn_2O_4$ single-phase samples to reveal their chemical and physical properties.

Acknowledgments

One of the authors (J. Akimoto) wishes to thank the late Prof. Shyun-iti Akimoto for his valuable suggestions

regarding the dense forms of the AB_2O_4 structure type using the high-pressure technique.

References

[1] J. Rodríguez-Carvajal, G. Rousse, C. Masquelier, M. Hervieu, Phys. Rev. Lett. 81 (1998) 4660–4663.
[2] J. Akimoto, Y. Takahashi, N. Kijima, Y. Gotoh, Solid State Ionics 172 (2004) 491–494.
[3] Y. Tomioka, A. Asamitsu, Y. Moritomo, H. Kuwahara, Y. Tokura, Phys. Rev. Lett. 74 (1995) 5108–5111.
[4] J. Akimoto, Y. Gotoh, K. Kawaguchi, Y. Oosawa, J. Solid State Chem. 96 (1992) 446–450.
[5] J. Akimoto, H. Takei, J. Solid State Chem. 79 (1989) 212–217.
[6] M.J. Geselbracht, L.D. Noailles, L.T. Ngo, J.H. Pikul, R.I. Walton, E.S. Cowell, F. Millange, D. O'Hare, Chem. Mater. 16 (2004) 1153–1159.
[7] J. Darriet, A. Vidal, Bull. Soc. Fr. Mineral. Cristallogr. 98 (1975) 374–377.
[8] Hk. Müller-Buschbaum, J. Alloy Compd. 349 (2003) 49–104.
[9] J.-P. Parant, R. Olazcuaga, M. Devalette, C. Fouassier, P. Hagenmuller, J. Solid State Chem. 3 (1971) 1–11.
[10] W.G. Mumme, Acta Crystallogr. B 24 (1968) 1114–1120.
[11] P. Barboux, J.M. Tarascon, F.K. Shokoohi, J. Solid State Chem. 94 (1991) 185–196.
[12] J. Akimoto, J. Awaka, Y. Takahashi, N. Kijima, M. Tabuchi, A. Nakashima, H. Sakaebe, K. Tatsumi, Electrochem. Solid-State Lett. 8 (2005) A554–A557.
[13] T. Irifune, K. Fujino, E. Ohtani, Nature 349 (1991) 409–411.
[14] M. Yutani, T. Yagi, H. Yusa, T. Irifune, Phys. Chem. Mineral. 24 (1997) 340–344.
[15] K. Tokiwa, H. Okumoto, S. Kono, S. Iga, K. Takemura, T. Watanabe, A. Iyo, Y. Tanaka, Int. J. Mod. Phys. B 19 (2005) 263–266.
[16] R. Hoppe, G. Brachtel, M. Jansen, Z. Anorg. Allgem. Chem. 417 (1975) 1–10.
[17] S.R. Hall, G.S.D. King, J.M. Stewart (Eds.), Xtal3.4 User's Manual, University of Western Australia, Lamb, Perth, 1995.
[18] E.F. Bertaut, F. Blum, G. Magnano, C.R. Acad. Sci. 241 (1955) 757–759.
[19] P.M. Hill, H.S. Peiser, J.R. Rait, Acta Crystallogr. 9 (1956) 981–986.
[20] B.F. Decker, J.S. Kasper, Acta Crystallogr. 10 (1957) 332.
[21] A.F. Reid, A.D. Wadsley, M.J. Sienko, Inorg. Chem. 7 (1968) 112–118.
[22] Hk. Müller-Buschbaum, D. Frerichs, J. Alloy Compd. 199 (1993) L5–L8.
[23] A.F. Wells, Models in Structural Inorganic Chemistry, Oxford University Press, Ely House, London, 1970, p. 102.
[24] K. Yamaura, Q. Huang, M. Moldovan, D.P. Young, A. Sato, Y. Baba, T. Nagai, Y. Matsui, E. Takayama-Muromachi, Chem. Mater. 17 (2005) 359–365.
[25] J. Akimoto, Y. Takahashi, Y. Gotoh, K. Kawaguchi, K. Dokko, I. Uchida, Chem. Mater. 15 (2003) 2984–2990.
[26] Y. Takahashi, J. Akimoto, Y. Gotoh, K. Dokko, M. Nishizawa, I. Uchida, J. Phys. Soc. Jpn. 72 (2003) 1483–1490.
[27] I.D. Brown, D. Altermatt, Acta Crystallogr. B 41 (1985) 244–247.
[28] J. Akimoto, Y. Takahashi, Y. Gotoh, S. Mizuta, Chem. Mater. 12 (2000) 3246–3248.
[29] M.M. Couffon, G. Rocher, J. Protas, C.R. Acad. Sci. 258 (1964) 1847–1849.
[30] G. Lepicard, J. Protas, Bull. Soc. Fr. Mineral. Cristallogr. 89 (1966) 318–324.
[31] H.G. Giesber, W.T. Pennington, J.W. Kolis, Acta Crystallogr. C 57 (2001) 329–330.
[32] C.D. Ling, J.J. Neumeier, D.N. Argyriou, J. Solid State Chem. 160 (2001) 167–173.
[33] E.F. Bertaut, P. Blum, Acta Crystallogr. 9 (1956) 121–126.
[34] M.P. Rogge, J.H. Caldwell, D.R. Ingram, C.E. Green, M.J. Geselbracht, T. Siegrist, J. Solid State Chem. 141 (1998) 338–342.
[35] S.J. Clarke, A.J. Fowkes, A. Harrison, R.M. Ibberson, M.J. Rosseinsky, Chem. Mater. 10 (1998) 372–384.
[36] W.R. Robinson, J. Solid State Chem. 9 (1974) 255–260.